Available online at www.sciencedirect.com
SCIENCE DIRECT®
PERGAMON
International Journal of Heat and Mass Transfer 46 (2003) 4319–4334
International Journal of HEAT and MASS TRANSFER
www.elsevier.com/locate/ijhmt

Numerical study of momentum and heat transfer in a pulsed plane laminar jet

Salwa Marzouk [a], Hatem Mhiri [a], Salem El Golli [a], Georges Le Palec [a,b,*], Philippe Bournot [a]

[a] *Laboratoire de Mécanique des Fluides et Thermique, Ecole Nationale d'Ingénieurs de Monastir, Route de Ouardanine, 5000 Monastir, Tunisie*

[b] *Equipe IMFT, Institut de Mécanique de Marseille, 60 rue Juliot Curie Technopole, de Chateau-Gombert, 13453 Marseille Cedex 13, France*

Received 23 July 2001; received in revised form 10 February 2003

Abstract

In this paper, we propose numerical solutions for a two-dimensional pulsed plane jet in unsteady laminar regime. At the exit of the nozzle, the pulsating flow is imposed with a uniform temperature T_0 and a velocity $u = u_0(1 + A\sin(\omega t))$. Two cases are considered: the free and the wall pulsed plane jet. For the wall jet case, the wall may either be considered adiabatic or subjected to a uniform temperature. Equations are treated with an appropriate finite difference method. The effect of the important governing parameters, such as the amplitude and the frequency of the pulsation, the Reynolds and Grashof numbers on the flow behavior are also investigated in detail. The results obtained show that the pulsation affects the flow in a vicinity region of the nozzle to reach the same asymptotic regime than the steady jet. The results also indicate that the initial development of the jet is considerably accelerated and the entrainment in the first diameters is enhanced.

1. Introduction

Due to the fact of the diversity of their aspects and their applications, typical jet flows present a constant interest. Indeed, many applications are met in industry such as, the pulverization, the cooling by film, aeronautic propellers, the welding, etc. [1].

Among the numerous works on this wide subject, some have treated the influence of an initial perturbation on the jet development. The motivations have been of two orders:

- On the practical plan, it consists on accelerating the jet expansion and increasing the exterior fluid entrainment.
- On the fundamental plan: the superposition of the periodic perturbation to the flow was proved to be a very fruitful method of investigation in order to understand the transition to the turbulence.

Most of works dealing with pulsating plane and axisymmetric jets are originally experimental, some of them [2–13] put into evidence the effect of an external perturbation in the appropriate kinematics of a free jet by considering a cyclic pulsation of the flow upstream the ejection, others used an acoustic emission generating a perturbation of the field of external static pressure.

The experimental work carried out based on the first approach showed that the pulsation accelerates considerably the initial development of the jet and clearly improves the diffusion and the entrainment in the first diameters [2,13]. This phenomenon is even observed for a low pulsation amplitude, since a value of 2% of the

* Corresponding author. Address: Laboratoire de Mécanique des Fluides et Thermique, Ecole Nationale d'Ingénieurs de Monastir, Route de Ouardanine, 5000 Monastir, Tunisie.

0017-9310/$ - see front matter © 2003 Elsevier Ltd. All rights reserved.
doi:10.1016/S0017-9310(03)00132-7

Nomenclature

A	flow pulse amplitude
C_f	friction coefficient, $C_f = \tau_w^*/\rho(v/x)^2$
e	width of the nozzle (m)
f	pulsation frequency (s^{-1})
Gr	Grashof number based on the width of the nozzle, $Gr = g\beta(T_0 - T_\infty)e^3/v^2$
Nu	local Nusselt number, $Nu = hx/\lambda$
$\overline{Nu}$	average Nusselt number
Pr	Prandtl number, $Pr = v/\alpha$
Re	Reynolds number, $Re = u_0 e/v$
Fr	Froude number, $Fr = Re^2/Gr = u_0^2/\rho\beta\Delta T_0 e$
St	Strouhal number, $St = fe/u_0$
t	time (s)
T	temperature (K)
u, v	dimensional axial and radial velocity ($m\,s^{-1}$)
U, V	dimensionless axial and radial velocity
x, y	dimensional axial and radial coordinate (m)
X, Y	dimensionless axial and radial coordinate

Greek symbols

α	thermal diffusivity of the fluid ($m^2\,s^{-1}$)
β	thermal expansion coefficient (K^{-1})
θ	dimensionless temperature, $\theta = (T - T_\infty)/(T_0 - T_\infty)$
v	kinematic viscosity of the fluid ($m^2\,s^{-1}$)
ρ	density of the fluid ($Kg\,m^{-3}$)
τ	dimensionless time
τ^*	shear stress (Pa)
ω	angular velocity, $\omega = 2\pi f$ ($rd\,s^{-1}$)

Subscripts

c	jet axis
m	modified quantity
w	wall
0	nozzle exit
∞	ambient environment

latter generates an increase in the entrainment rate of 20% compared to the case of the nonpulsed jet [7].

The periodic disturbances are amplified at a distance which is estimated at two to three times of the nozzle diameter, then decrease to disappear, at a distance close to 10 diameters beyond the degenerated vortex and are accompanied by a very significant increase in the turbulent intensity, so a transfer of energy thus takes place of the jet periodic structure towards the turbulence.

The second approach based on the perturbation of the external static pressure field was adopted by several researchers, so for the jet axisymmetric case [7,8] used a loudspeaker to create acoustic waves having a detectable amplitude in the nozzle. They noticed that for the Reynolds numbers about of 10^4, instabilities occurred closer to the nozzle. These instabilities develop in axisymmetric vortices-ring which very often meet at a close distance from 2 to 3 nozzle diameters and give rise to large structures which size has the bulk order of the jet width. After 5 diameters, these structures become three-dimensional and lose their axisymmetric character.

The influence of the pulsation on the heat transfer was treated essentially for the case of a pulsed axisymmetric jet impinging a horizontal plate [9,14–18]. It was shown that, for very low amplitudes and Strouhal numbers, the Nusselt number is independent of the amplitude and the frequency of pulsation [15], on the other hand, an increase in these last ($St > 10^{-2}$ and $A > 40\%$), strongly influences the thermal transfer [17].

To our knowledge the energy transfer in a wall plane jet case subjected to a controlled perturbation was treated experimentally by Zhou et al. [19]. These authors considered a sinusoidal perturbation of the pressure, they found that for an amplitude of pulsation of 5% and for a Strouhal number equal to 9.5×10^{-3}, the friction coefficient for the distances X ranging between 100 and 200 decreases approximately by 7% compared to the nonpulsed case. They noticed also that for X less than 100, the intensity of the longitudinal velocity fluctuating component increases in the vicinity of the wall compared to that of the steady jet.

This brief review of the works carried out about the pulsed jets shows that this type of flow was especially the object of experimental studies; the complexity of present phenomena gives back a purely difficult theoretical analysis of the problem otherwise it can be presented under a simplified form. The existence of such difficulty opens an interesting field although it is delicate when using numerical resolutions.

In this context, and in order to determine if a numerical study would allow to find the main experimental observations, we propose in this work numerical solutions for the two-dimensional pulsed plane jet. Two cases are examined in transient laminar regime: the free pulsed jet (Fig. 1(a)) and the wall pulsed jet (Fig. 1(b)). For the wall jet case, the wall may be considered either adiabatic or subjected to a uniform temperature.

The numerical results describe the effect of several parameters such as the amplitude and the frequency of pulsation as well as the Reynolds and the Grashof numbers on the dynamical and thermal characteristics of the pulsed free and wall jet.

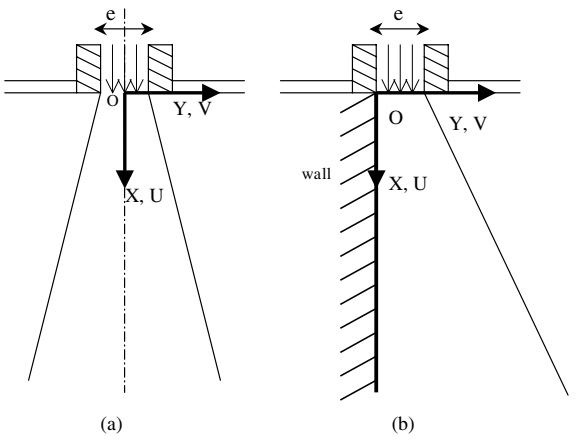

Fig. 1. Coordinates system (a) free jet (b) wall jet.

2. Mathematical formulation

2.1. Assumptions

We consider vertical jet issues from a rectangular plane nozzle with small dimensions in comparison to enclosure, or the ambient environment in which emerges the flow, the jet and the ambient environment are constituted of the same fluid. For low values considered of amplitude and frequency of pulsation, the flow is supposed to be of boundary layer type.

We also assume that the width of the nozzle is very large as compared to its thickness in order to neglect the edge effects and to have a two-dimensional problem.

For the used range of the Grashof numbers, the fluid density varies linearly with the temperature in the term containing the buoyancy force, it is considered constant elsewhere, according to the Boussinesq assumptions.

The pressure is supposed constant in the jet. This latter is submitted to a longitudinal and periodic perturbation to an unidirectional character of the ejection velocity. The flow is supposed to be laminar and unsteady.

2.2. Governing equations

With the above assumptions, in a Cartesian coordinates system, the mass, momentum and energy equations, in properly dimensionless form, can be written as follows:

$$\frac{\partial U}{\partial X}+\frac{\partial V}{\partial Y}=0 \tag{1}$$

$$\frac{\partial U}{\partial \tau}+U\frac{\partial U}{\partial X}+V\frac{\partial U}{\partial Y}=\frac{1}{Re}\frac{\partial^2 U}{\partial Y^2}\pm\gamma\frac{1}{Fr}\theta \tag{2}$$

$$\frac{\partial \theta}{\partial \tau}+U\frac{\partial \theta}{\partial X}+V\frac{\partial \theta}{\partial Y}=\frac{1}{RePr}\frac{\partial^2 \theta}{\partial Y^2} \tag{3}$$

The dimensionless parameters which appear in the above equations are *Re*, *Pr* and *Fr* numbers defined as

$$Re=\frac{u_0 e}{v};\quad Pr=\frac{v}{\alpha},\quad Fr=\frac{Re^2}{Gr}=\frac{u_0^2}{\rho\beta(T_0-T_\infty)e}$$

The Eqs. (1)–(3) are obtained by considering the following dimensionless quantities:

$$(X,Y)=\frac{(x,y)}{e},\quad (U,V)=\frac{(u,v)}{u_0},\quad \theta=\frac{T-T_\infty}{T_0-T_\infty},\quad \tau=\frac{tu_0}{e} \tag{4}$$

u_0 and T_0 respectively being the velocity and the temperature of the fluid at the nozzle exit.

γ takes values 0 and 1, for $\gamma=0$ the first two equations formulate the isothermal plane jets. For the non-isothermal case ($\gamma=1$), the + sign represents the case of an ascending heated or descending cold jet, whereas the − sign represents the case of a descending heated or ascending cold jet. These equations are written in a Cartesian coordinate system such as the axes origin (O) is located in the middle of the exit section for a free jet, and on the plate for a wall jet (Fig. 1).

The associated dimensionless boundary and ejection conditions to the Eqs. (1)–(3) are described as

- For free jet:

$$X>0,\quad \begin{cases} Y=0; & V(X,0,\tau)=0; \\ & \frac{\partial U(X,0,\tau)}{\partial Y}=0; \quad \frac{\partial \theta(X,0,\tau)}{\partial Y}=0 \\ Y\mapsto\infty; & U(X,Y,\tau)\to 0; \quad \theta\to 0 \end{cases} \tag{5}$$

$$X=0,\quad V(0,Y,\tau)=0$$

$$\text{and}\quad \begin{cases} \text{if } 0\leqslant Y<0.5 \\ \qquad U(0,Y,\tau)=1+A\sin(2\pi St\tau) \\ \qquad \theta(0,Y,\tau)=1 \\ \text{if } Y\geqslant 0.5 \\ \qquad U(0,Y,\tau)=0 \\ \qquad \theta(0,Y,\tau)=0 \end{cases} \tag{6}$$

- For wall jet:

$$\text{Pour } X>0\quad \begin{cases} Y=0; \quad V(X,0,\tau)=0; \quad U(X,0,\tau)=0 \\ Y\to\infty; \quad U(X,Y,\tau)\to 0 \quad \theta(X,Y,\tau)\to 0 \end{cases} \quad \text{and} \quad \begin{cases} \frac{\partial \theta(X,0,\tau)}{\partial Y}=0 & \text{adiabatic wall} \\ \theta(X,0,\tau)=1 & \text{isothermal wall} \end{cases} \tag{7}$$

$$X=0,\quad V(0,Y,\tau)=0,\quad U(0,Y,\tau)=0$$

$$\text{and}\quad \begin{cases} \text{if } 0<Y<1 \\ \qquad U(0,Y,\tau)=1+A\sin(2\pi St\tau) \\ \qquad \theta(X,Y,\tau)=1 \\ \text{if } Y\geqslant 1 \\ \qquad U(0,Y,\tau)=0 \\ \qquad \theta(0,Y,\tau)=0 \end{cases} \tag{8}$$

In this work the temperature and the velocity fields of a steady jet are used as initial conditions associated to Eqs. (2) and (3).

2.3. Numerical method

In this work, Eqs. (1)–(3) associated to the conditions Eqs. (5) and (6) for a pulsed free jet, and Eqs. (7) and (8) for a pulsed wall jet, are solved numerically by a finite difference method using a staggered grid, so that the space discretization of the transport equations is carried out at the node $(i+1/2,j)$, i and j respectively referring nodes along the X and Y axis (Fig. 2), whereas the continuity equation is discretized at the node $(i+1/2,j+1/2)$. The temporal discretization of the equations is also carried out by a finite difference scheme. The iterative method used is that of the non-linear Gauss–Seidel method which is a successive approximation method [20].

The equation of continuity is discretized at the node $(i+1/2,j+1/2)$ and at the time $k+1$ is written as follows:

$$\frac{1}{2}\left(\frac{U^{k+1}_{i+1,j}-U^{k+1}_{i,j}}{\Delta X}+\frac{U^{k+1}_{i+1,j+1}-U^{k+1}_{i,j+1}}{\Delta X}\right)+\frac{1}{2}\left(\frac{V^{k+1}_{i+1,j+1}-V^{k+1}_{i+1,j}}{\Delta Y}+\frac{V^{k+1}_{i,j+1}-V^{k+1}_{i,j}}{\Delta Y}\right)=0$$

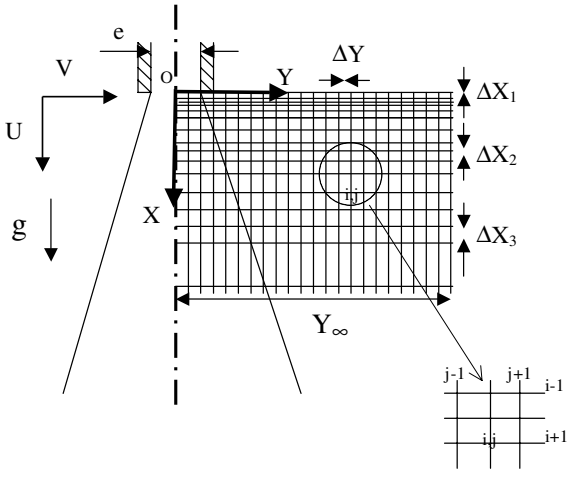

Fig. 2. Longitudinal X and transversal Y space steps definition.

The momentum and energy equations are discretized at the node $(i+1/2,j)$ and at the time $k+1$, and are written as follows:

$$\left(\frac{U^{k+1}_{i+1/2,j}-U^{k}_{i+1/2,j}}{\Delta\tau}\right)+U^{k+1}_{i+1/2,j}\left(\frac{U^{k+1}_{i+1,j}-U^{k+1}_{i,j}}{\Delta X}\right)+V^{k+1}_{i+1/2,j}\frac{1}{2}\left(\frac{U^{k+1}_{i+1,j+1}-U^{k+1}_{i+1,j-1}}{2\Delta Y}+\frac{U^{k+1}_{i,j+1}-U^{k+1}_{i,j-1}}{2\Delta Y}\right)=\frac{1}{2Re}\left(\frac{U^{k+1}_{i+1,j+1}+U^{k+1}_{i+1,j-1}-2U^{k+1}_{i+1,j}}{\Delta Y^2}+\frac{U^{k+1}_{i,j+1}+U^{k+1}_{i,j-1}-2U^{k+1}_{i,j}}{\Delta Y^2}\right)\pm\gamma\frac{1}{Fr}\theta^{k+1}_{i+1/2,j}$$

$$\left(\frac{\theta^{k+1}_{i+1/2,j}-\theta^{k}_{i+1/2,j}}{\Delta\tau}\right)+U^{k+1}_{i+1/2,j}\left(\frac{\theta^{k+1}_{i+1,j}-\theta^{k+1}_{i,j}}{\Delta X}\right)+V^{k+1}_{i+1/2,j}\frac{1}{2}\left(\frac{\theta^{k+1}_{i+1,j+1}-\theta^{k+1}_{i+1,j-1}}{2\Delta Y}+\frac{\theta^{k+1}_{i,j+1}-\theta^{k+1}_{i,j-1}}{2\Delta Y}\right)=\frac{1}{2RePr}\left(\frac{\theta^{k+1}_{i+1,j+1}+\theta^{k+1}_{i+1,j-1}-2\theta^{k+1}_{i+1,j}}{\Delta Y^2}+\frac{\theta^{k+1}_{i,j+1}+\theta^{k+1}_{i,j-1}-2\theta^{k+1}_{i,j}}{\Delta Y^2}\right)$$

with $B^{k+1}_{i+1/2,j}=(B^{k+1}_{i+1,j}+B^{k+1}_{i,j})/2$, where B stands for U, θ and V.

This method used in previous works for the study of steady free jets [21,22] or for a flow occurring in a channel [23], was adopted for stability numerical reasons compared to a non-staggered grid discretization. The grid considered is rectangular (Fig. 2); indeed, the calculation step is taken very thin in the nozzle vicinity ($\Delta X_1=10^{-4}$ for $0\leqslant X\leqslant 3$); Then, a little further, we increase its value ($\Delta X_2=10^{-3}$ for $3<X\leqslant 10$) and finally we consider a larger step for higher longitudinal coordinates ($\Delta X_3=10^{-2}$ for $X>10$) in order to be able to go further in the jet. An iterative "line by line" scan method is used according to direction X, in order to save convergence time.

In the transversal direction, the used mesh is uniform, the calculation step is constant ($\Delta Y=0,01$) and its specified value ensures a sufficient number of points N in this direction to take into account the jet "blooming". The distance $Y_\infty=(N-1)*\Delta Y$ (Fig. 2) is of the order of 18 for the free pulsed jet case while it is worth 35 for the wall pulsed jet (which means that 1800 and 3500 points, respectively, are necessary along the direction Y).

The time resolution was as such one pulsating period was divided by 120 time steps. The sensitivity of the calculated results to the grid interval, time step and accuracy level in the convergence criteria was verified by repeating calculations. The computational parameters that were selected in the present work were found to

yield satisfactory results in the grid—and time step—convergence tests.

After introducing the arbitrary fields, calculations are executed by using first the algebraic momentum equation to determine the longitudinal velocity U for all the mesh node. the algebraic continuity equation allows us then to calculate the transversal velocity V. Thus the temperature is finally determined from the algebraic energy equation by using the obtained values of the velocity. The resulting finite difference equations are solved by the Gauss–Siedel elimination method associated with the successful over relaxation technique. The iterative process is terminated when the following convergence criterion $|(\phi^{m+1} - \phi^m)/\phi^m| \leqslant 10^{-5}$ is verified for each grid node at every time step; m being the iteration number and ϕ represents U and T.

3. Results and discussion

3.1. Free pulsed jet in a mixed convection regime

In this part, we will examine in a laminar regime, the influence of the pulsation on the dynamic and thermal quantities of a free heated plane jet. Our results are presented in the case of the air ($Pr = 0.71$) and the jet is considered either an ascending heated or a descending cold jet ($\gamma = 1$). The results presented are obtained in a mixed convection mode.

It would be interesting in a first stage to analyze the disturbance influence on the temporal evolution of the principal flow parameters.

Thus, we present on Fig. 3 the temporal evolution of the centerline velocity at various sections and for various pulsation amplitudes values, the Strouhal number is fixed at a value equal to 0.3. In the vicinity of the nozzle ($X = 3$), the velocity always keeps a sinusoidal profile of identical period to that of the pulsation, then, and for $X = 6$ the flow still consists of coherent puffs of periods close to the pulsation period but having a non-periodic part (flat) because of the distance already traversed from the nozzle. For $X = 12$, the sinusoidal profile disappeared, but a trace of the disturbance still persists in the form of a velocity maximum.

For $X = 30$, the centerline velocity presents a flat part which extends until $t = 5T$; this latter is the time put by the disturbance to traverse the distance $X = 30$. In addition, the same figure puts in evidence the presence of a sinusoidal oscillation of low amplitude which diminishes downstream from the nozzle with time.

Fig. 4 shows the temporal evolution of the centerline velocity to various sections and for various Strouhal numbers values. It is noticed that for a low Strouhal number ($St = 0.1$) velocity keeps a sinusoidal profile on very high distances to the nozzle.

For higher pulsation frequencies (high Strouhal numbers), the sinusoidal structure of the flow is of a low amplitude and quickly loses its identity by fusion under the effect of molecular viscosity. This phenomenon was already found by Acton [27] in the case of a disturbed axisymmetric turbulent jet for the same Strouhal numbers and the pulsation amplitude considered in this work.

For the temporal evolution of the centerline temperature for various pulsation amplitudes (Fig. 5) and for various Strouhal numbers (Fig. 6), we observed the same phenomena as those noted for centerline velocity on the jet axis.

In a second stage, we wanted to examine the disturbance influence on the instantaneous evolution (for a fixed time) of characteristic quantities of the flow. All results are presented for $\omega t = 9\pi/2$ what corresponds to $t = 9T/4$.

In order to compare our results in a mixed convection mode ($Fr = 20$) with those obtained by Yu et al. [26] and Mhiri et al. [21] for the case of a steady plane jet, we present on Fig. 7, the longitudinal distributions of the modified centerline velocity given by the relation $U_{cm} = U_c(Fr/Re)^{0.25}$ (Fig. 7(a)) and the modified centerline temperature expressed as $\theta_{cm} = \theta_c(Fr/Re)^{0.25}$ (Fig. 7(b)), according to the modified distance X_m defined by $X_m = X(1/Fr^3Re)^{0.25}$. We notice that the obtained results coincide with those of [21] and [26] only in the plume region (far from the nozzle). A significant difference between our results and those established by Yu et al. [26] is observed in the jet region (in the vicinity of the nozzle) and intermediate region. Indeed, these authors have associated to Eqs. (1)–(3), two integration constraints which express the conservation of momentum and energy, these constraints replace the dynamic (Eq. (5)) and the thermal (Eq. (6)) ejection conditions for the equations resolution. It was then shown in a previous work [21], that these constraints can be verified for any emission profiles (uniform, parabolic, etc.). The approach considered by Yu et al. [26] which consists in ignoring the dynamic and thermal conditions at the exit of the nozzle, thus explains the observed variation between their results and ours in the jet region and the intermediate zone.

This same figure enables us to notice that the modified centerline velocity and temperature of the pulsed jet presents fluctuations in the jet zone and in the intermediate region, the amplitude of these fluctuations is higher for small Reynolds numbers, which enables us to deduce that the impact of the pulsation is more significant when the flow is in a slow movement. This was already observed by Siegl in the case of a pulsating channel flow [24,25]. It is also noticed that the fluctuations created by the pulsation persist at larger distances for small Reynolds numbers and that the pulsation does not affect the flow in the plume zone, in the latter our results

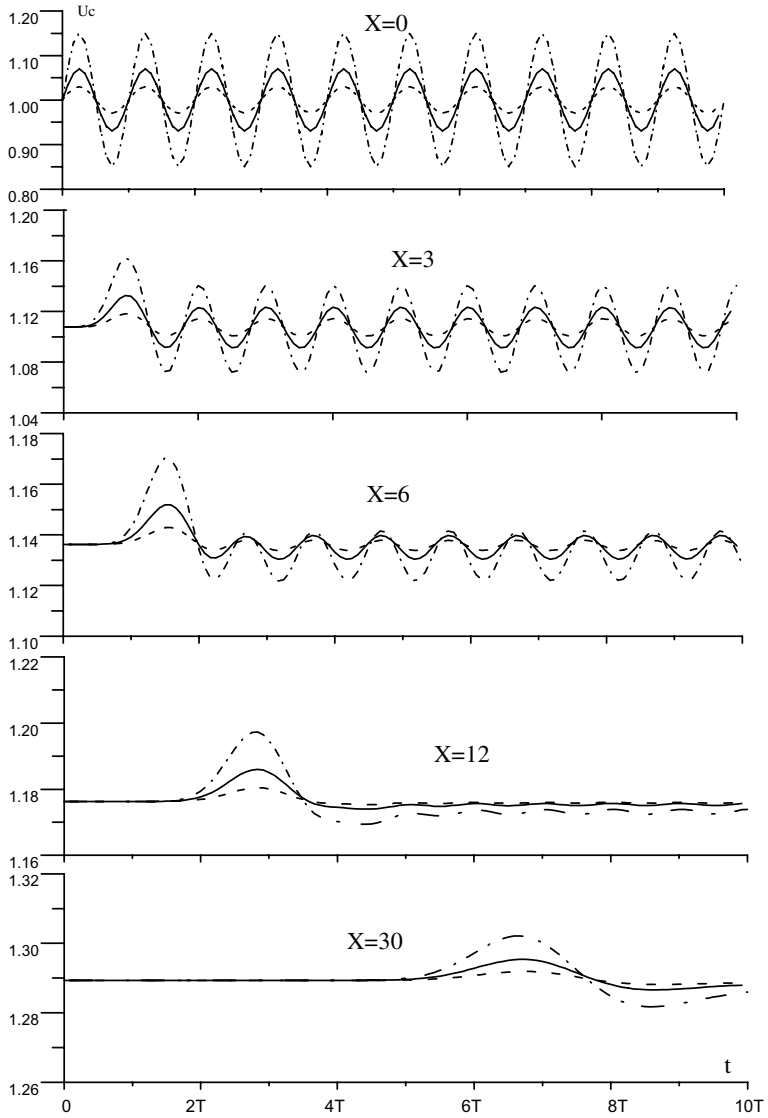

Fig. 3. Temporal evolution of the centerline velocity for $Re = 100$; $Fr = 20$; $St = 0.3$; - - - $A = 3\%$; — $A = 7\%$; –·–·–·– $A = 15\%$.

coincide well with those of Mhiri et al. [21] and Yu et al. [26].

To analyze the influence of the pulsation (amplitude of pulsation and Strouhal number) on the characteristic quantities of the flow, we have respectively fixed the Reynolds number and that of Froude at values equal to 100 and 20 that corresponds to a mixed convection mode.

Fig. 8 shows the longitudinal distribution of the jet centerline velocity for various amplitudes of pulsation (Fig. 8(a)) and for various Strouhal numbers (Fig. 8(b)). We notice that the introduction of a disturbance to the flow involves the appearance of oscillations which amplitudes increase with that of the pulsation (Fig. 8(a)). These oscillations disappear completely at the same distance equal to 14 times of the nozzle width for the various pulsation amplitudes, beyond this distance the obtained centerline velocity for a pulsed jet is the same one as that established by a permanent jet (nonpulsed) for all the considered pulsation amplitudes.

When we increase the pulsation frequency (Strouhal number), the oscillations appear in distances more closer to the nozzle (Fig. 8(b)). On the other hand, the evolution towards the asymptotic mode of the permanent jet is reached more quickly. Indeed, these oscillations disappear more quickly for high Strouhal numbers whereas they persist at larger distances for lower pulsation frequencies (for $St = 0.1$, these oscillations disappear at a

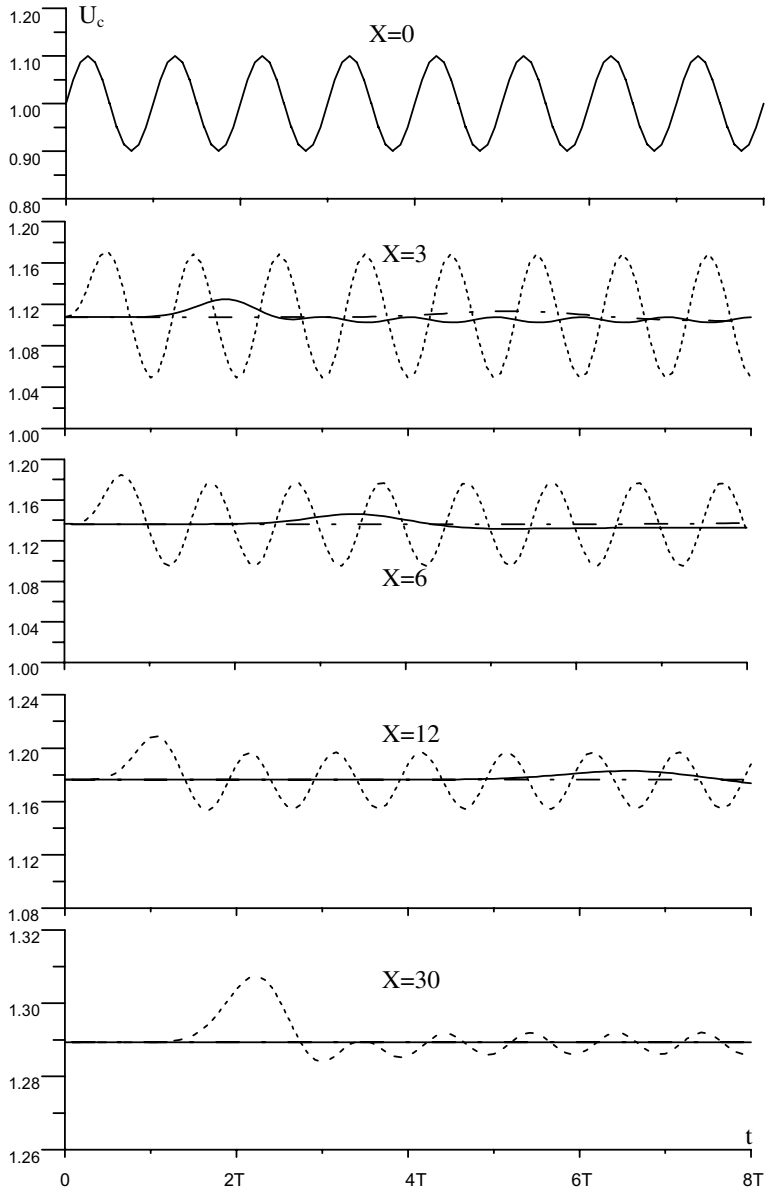

Fig. 4. Temporal evolution of the centerline velocity for $Re = 100$; $Fr = 20$; $A = 10\%$; --- $St = 0.1$; — $St = 0.7$; $-\cdot-\cdot-\cdot-$ $St = 2$.

distance closer to $X = 40$). This result was already put into in evidence by Mladin and Zumbrunnen [9] in the region closer to the nozzle in the case of a pulsed jet impacting a heated plate.

To analyze the effect of the heating on the evolution of the disturbance in the flow, we traced on Fig. 9 the longitudinal distribution of the centerline velocity (Fig. 9(a)) and the centerline temperature (Fig. 9(b)) for various Froude numbers. According to this figure, we notice that the influence of Froude number on the evolution of these greatnesses is observed only for values of X lower than 20. We notice that for the pulsed jet, the centerline velocity and temperature present fluctuations with regard to those of the permanent jet. On this same figure we deduce that the increase of thermal gradient between the jet and the ambient environment (low Froude numbers) involve oscillations of higher amplitudes accompanied by a widening of the dissipation region of these fluctuations. The heating is thus a significant factor for the study of the behavior of a pulsed jet.

Fig. 10 presents the evolution of the limit value of the transverse component velocity $V\ell$ (for $Y \mapsto \infty$). We notice on Fig. 10(a) that the variation of the pulsation

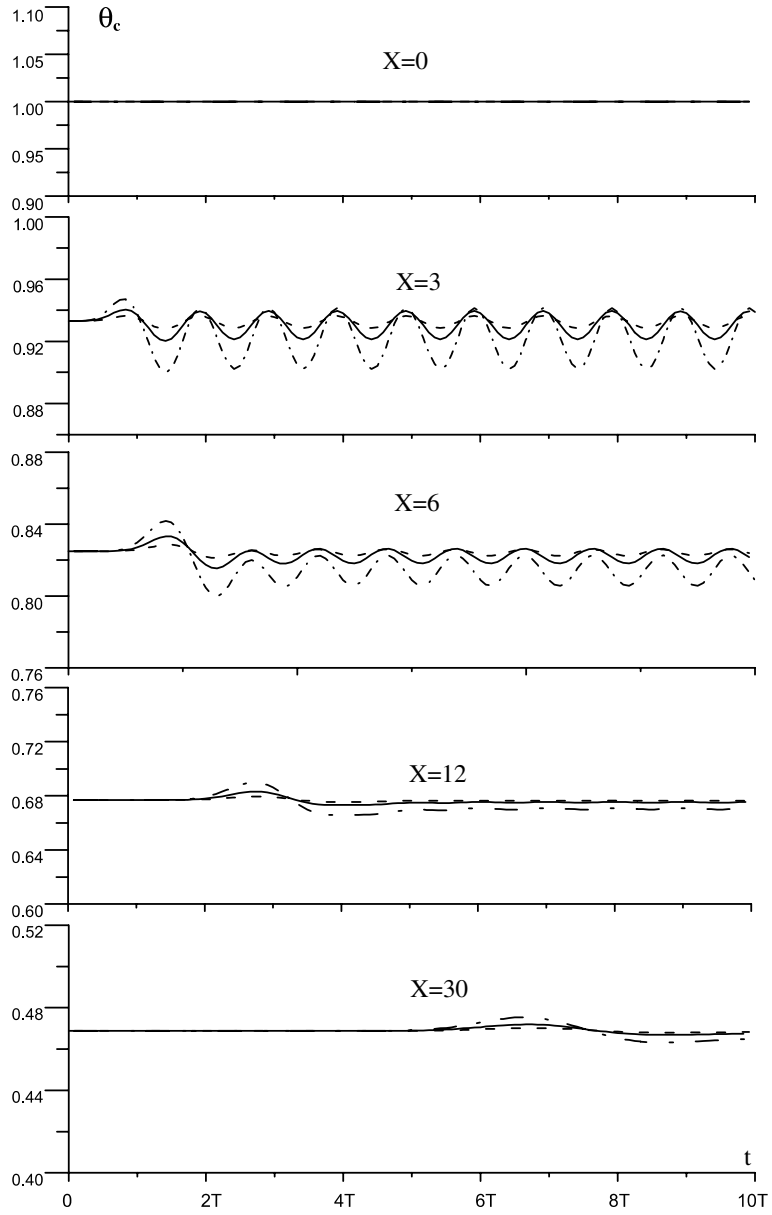

Fig. 5. Temporal evolution of the centerline temperature for $Re = 100$; $Fr = 20$; $St = 0.3$; - - - $A = 3\%$; — $A = 7\%$; – · – · – · – $A = 15\%$.

amplitude generates a contribution of maximum air in the immediate vicinity of the nozzle (at a distance close to $X = 1.5$), for the all considered amplitudes. This entrainment is higher since the amplitude of pulsation is large. We notice also that the pulsation amplitude does not affect the length of the region where the fluctuations of the limit transverse velocity appear.

Fig. 10(b) shows that when we vary the pulsation frequency, the maximum of the entrainment is observed at a distance which depends on a Strouhal number. Indeed for the great values of this latter ($St = 2$), the maximum air contribution is observed in the immediate vicinity of the ejection nozzle ($X \approx 0.2$), on the other hand for a low value of the pulsation frequency ($St = 0.1$), the maximum air contribution while being lower, is situated at a distance far from the nozzle ($X = 4$).

Fig. 10 also shows that for the permanent jet, the driving velocity is always negative, whereas for the pulsed jet it oscillates between negative and positive values which allows us to think that the pulsation favors the creation of vortices on the jet edges, the latter are

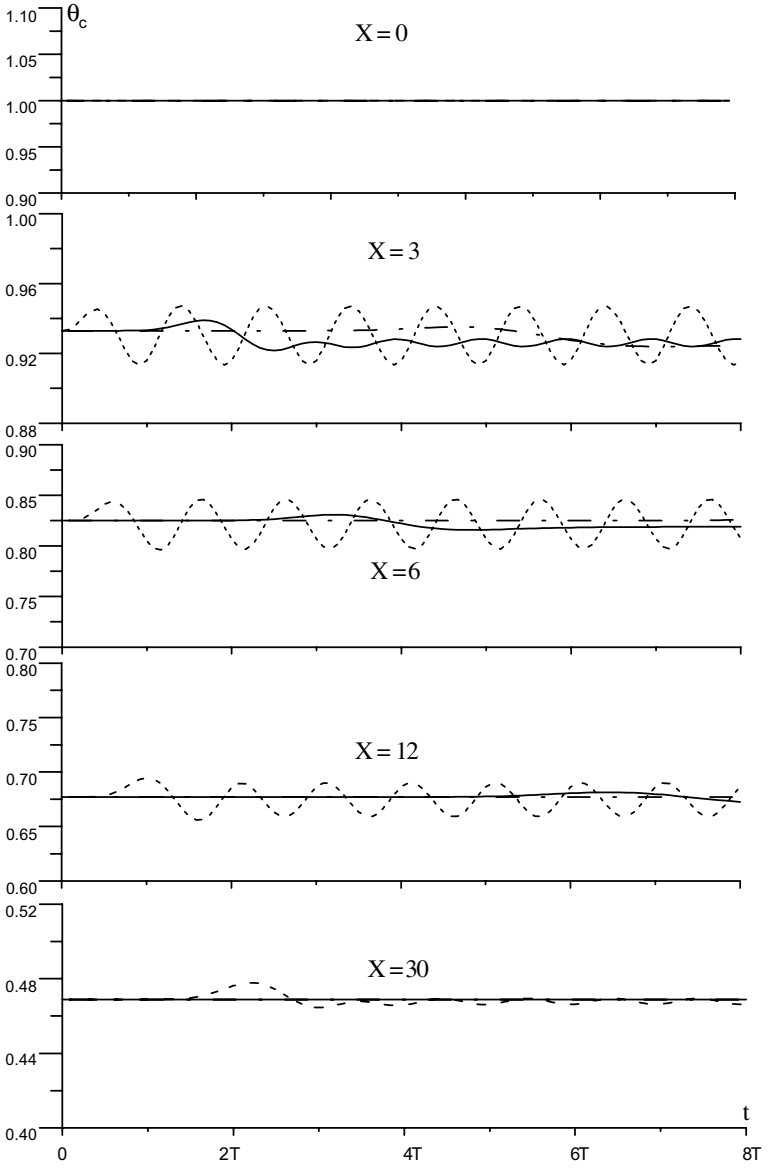

Fig. 6. Temporal evolution of the centerline temperature for $Re = 100$; $Fr = 20$; $A = 10\%$; - - - $St = 0.1$; — $St = 0.7$; –·–·–·– $St = 2$.

present in the flow in a region located between the nozzle and $X = 14$ when we vary the pulsation amplitude (Fig. 10(a)), this result was already indicated for the low values of the Strouhal number by Crow and Champagne [7]. When the pulsation frequency is increased, these vortices appear in the immediate vicinity of the nozzle, on the other hand for the low Strouhal numbers they appear further and persist on distances far away from the ejection nozzle (Fig. 10(b)).

The influence of the pulsation on the centerline temperature of the jet is given in Fig. 11, we notice that the disturbance of the ejection velocity affects also the thermal field since the temperature presents oscillations in the first jet (Fig. 11). The identical establishment to those expressed for longitudinal centerline velocity can be carried out for the evolution of this quantity. Indeed, we notice that the variation of the pulsation amplitude has no effect on the distance from which the oscillations disappear (Fig. 11(a)). On the other hand, the increase of the Strouhal number (Fig. 11(b)) generates a faster appearance of these oscillations in the nozzle vicinity and accelerates the evolution towards a permanent regime. It is however necessary to say that the pulsation tends to cool the

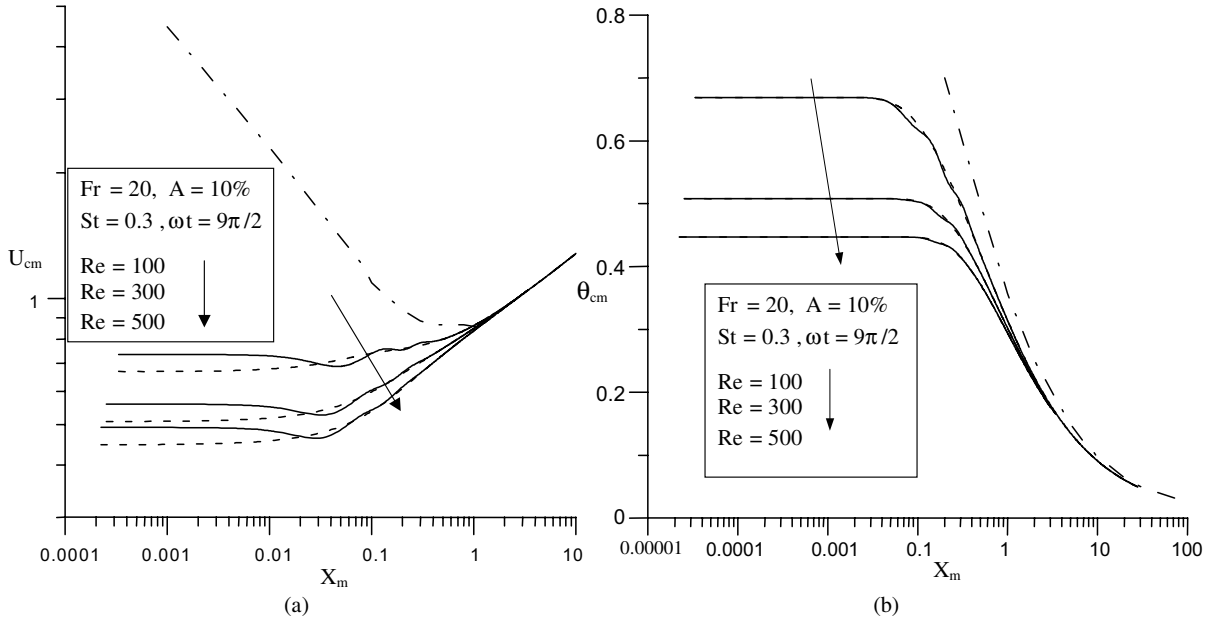

Fig. 7. Influence of Reynolds numbers on longitudinal distribution of the modified: (a) centerline velocity, (b) centerline temperature; --- results of [21]; –·–·–·– results of [26].

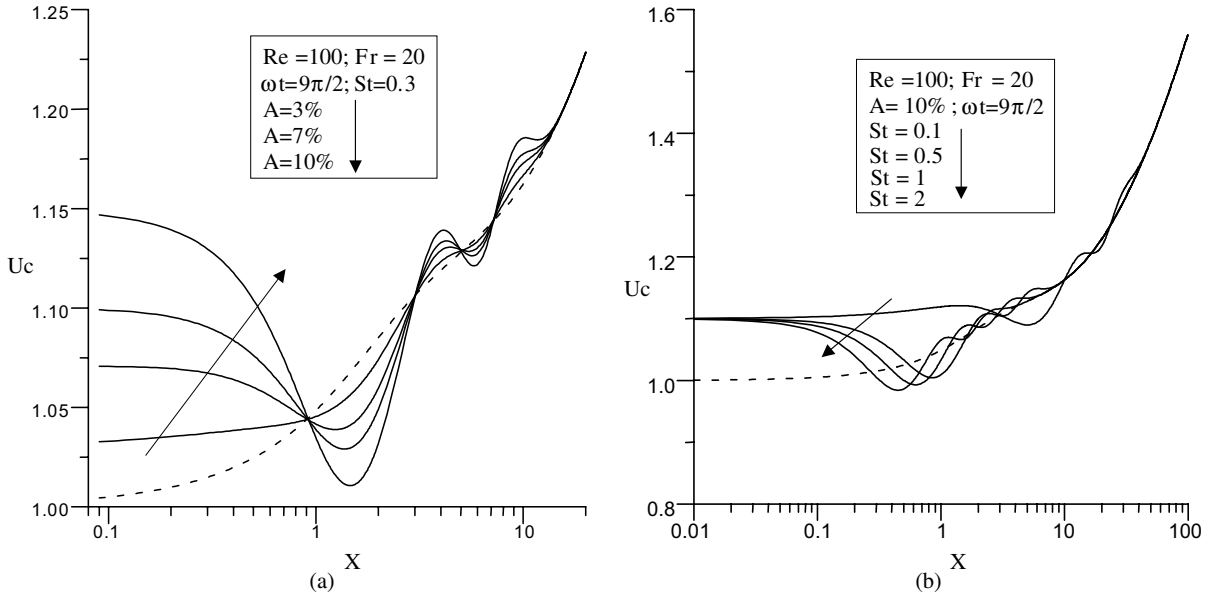

Fig. 8. Longitudinal distribution of the centerline velocity: (a) Influence of pulse amplitude, (b) influence of Strouhal number; --- results of [21].

jet in the first diameters, indeed, Fig. 10 shows us that in this region, the introduction of a disturbance increases the drive of the surrounding air and consequently the thermal exchange with the ambient conditions.

3.2. Pulsed parietal jet in a mixed convection regime

3.2.1. Adiabatic wall

In this part, we present an analysis on the behavior of a pulsed parietal plane jet which develops tangentially

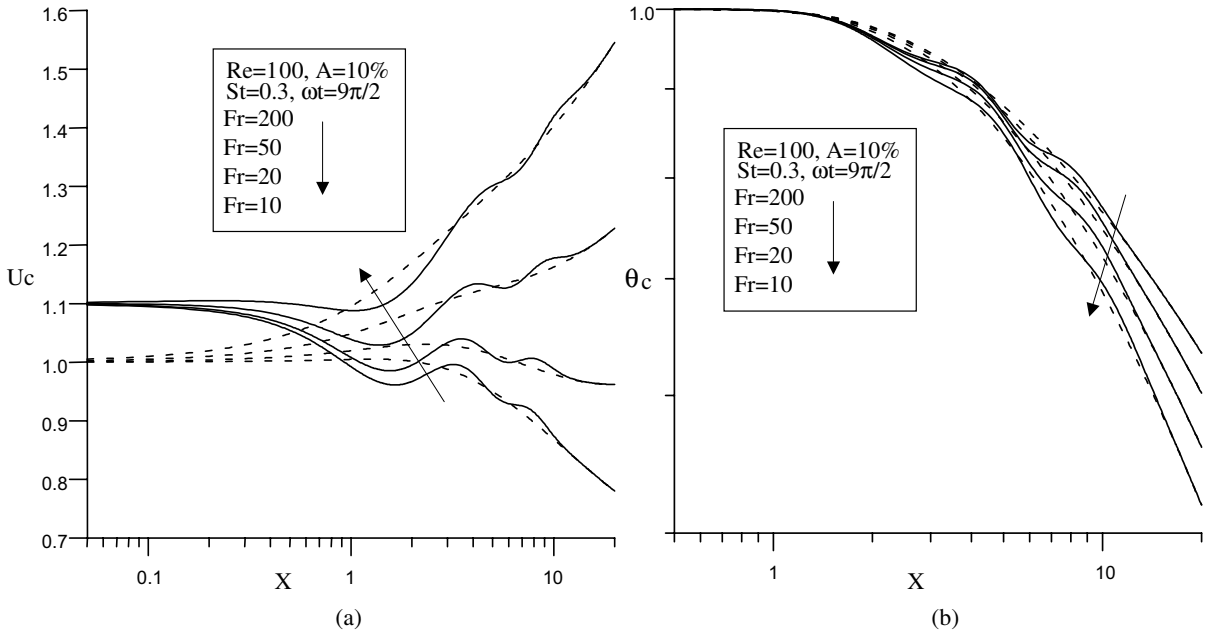

Fig. 9. Influence of Froude numbers on longitudinal distribution of the (a) centerline velocity, (b) centerline temperature; - - - results of [21].

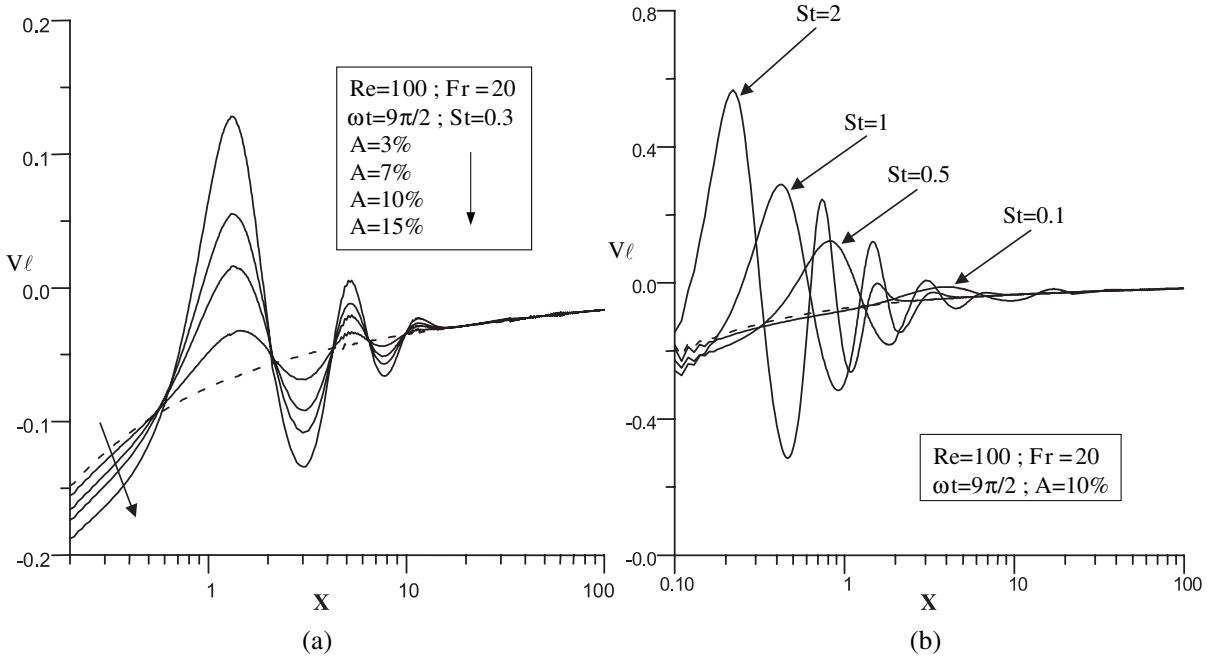

Fig. 10. Longitudinal distribution of the limit transverse velocity: (a) influence of pulse amplitude, (b) influence of Strouhal number, - - - results of [21].

with an adiabatic wall. The results obtained are presented in the case of the air ($Pr = 0.71$) for $\gamma = 1$ (ascending heated jet or descending cold jet) and in a mixed convection regime. We are interested particularly in the

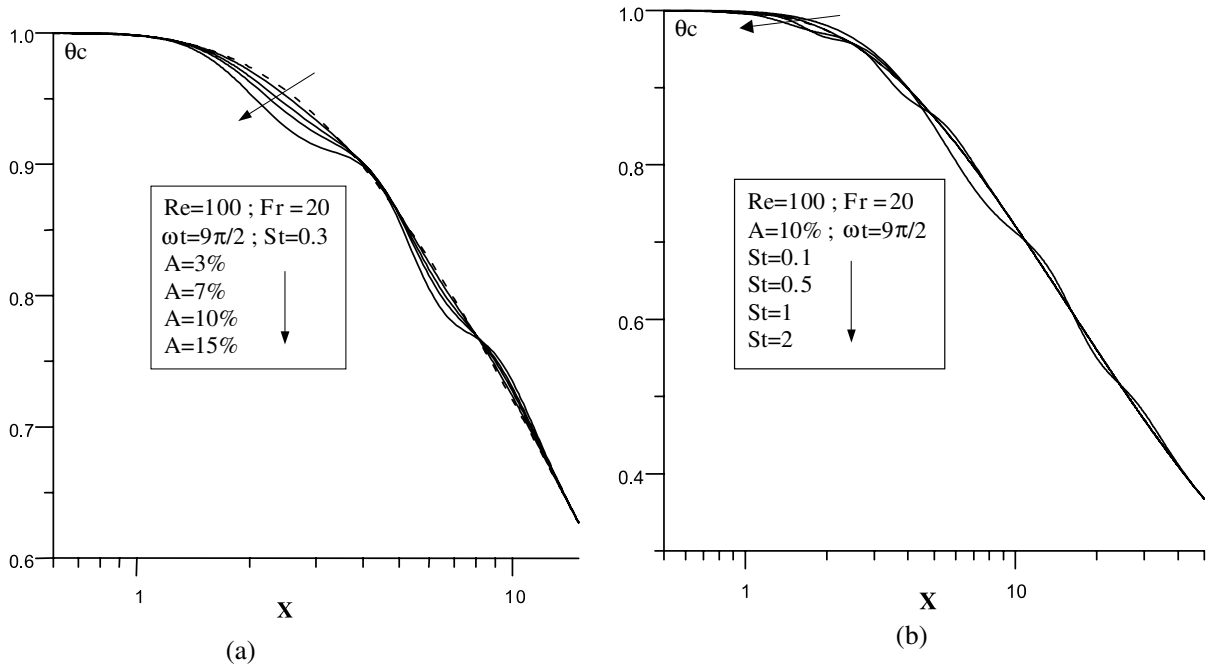

Fig. 11. Longitudinal distribution of the centerline temperature: (a) influence of pulse amplitude, (b) influence of Strouhal number; - - - results of [21].

pulsation amplitude and the Strouhal number influence on the shear stress and on the thermal quantities of the flow.

The dimensionless shear stress τ^* is defined as

$$\tau^* = \frac{\tau_w^*}{\rho(v/e)^2} = Re\left.\frac{\partial U}{\partial Y}\right|_{Y=0} \tag{9}$$

In order to compare our results with those of Yu et al. [26] and of Mhiri et al. [21] in the case of a parietal plane jet tangentially developing with an adiabatic wall, we present in Fig. 12 the modified shear stress defined by $\tau_m^* = \tau^*(Fr^5/Re^{12})^{1/7}$ according to the modified longitudinal distance given by $X_m = X/(Fr^4Re^3)^{1/7}$; the same results are obtained with those proposed by Yu et al. [26] and Mhiri et al. [21]. As for the free jet case, it is observed only in the region of the thermally established regime (plume zone), in this zone the pulsation has no more influence on the flow.

The evolution of the modified shear stress is given in Fig. 12(a) according to the modified longitudinal distance X_m for various amplitudes of pulsation and by maintaining the other fixed parameters ($St = 0.3$; $Re = 100$; $Fr = 20$), this figure shows that for a low amplitude ($A = 3\%$), the pulsation does not influence this greatness and the results obtained for a parietal pulsed jet are practically similar to those established for the permanent parietal jet. On the other hand, an increase in the pulsation amplitude causes an increase of the shear stress in the jet region (in the nozzle vicinity). This is completely predictable since a higher pulsation amplitude involves a more important longitudinal velocity gradient at the wall, indeed the ejection velocity being a sinusoidal function, for $\omega t = 9\pi/2$, this velocity is higher than that of a permanent jet.

The longitudinal distribution of the modified shear stress is presented for various Strouhal number values in Fig. 12(b). The results are obtained for $Re = 100$, $Fr = 20$ and $A = 10\%$. This figure shows that this pulsation frequency does not affect the evolution of this greatness in the immediate vicinity of the nozzle ($X_m < 10^{-3}$ which corresponds to $X \cong 0.1$), this being predictable since the ejection velocity is constant for $\omega t = 9\pi/2$ and for various Strouhal numbers values. The effect of the periodic disturbance on the shear stress is observed only in one region ranging between $X_m \cong 0.001$ and $X_m \cong 0.1$ that corresponds to a zone located between $X \cong 0.1$ and $X \cong 8$.

The longitudinal distribution of the wall temperature θ_w of the pulsed parietal jet is presented in mixed convection regime for various pulsation amplitudes (Fig. 13(a)) and for various Strouhal numbers (Fig. 13(b)).

The pulsation amplitude influences the wall temperature in a region ranging between $X = 3$ and $X = 10$, in this zone this quantity presents a small reduction compared to its permanent homologue, this is due to an increase in the entrainment of the surrounding air on the jet edges which increases the heat exchange between the

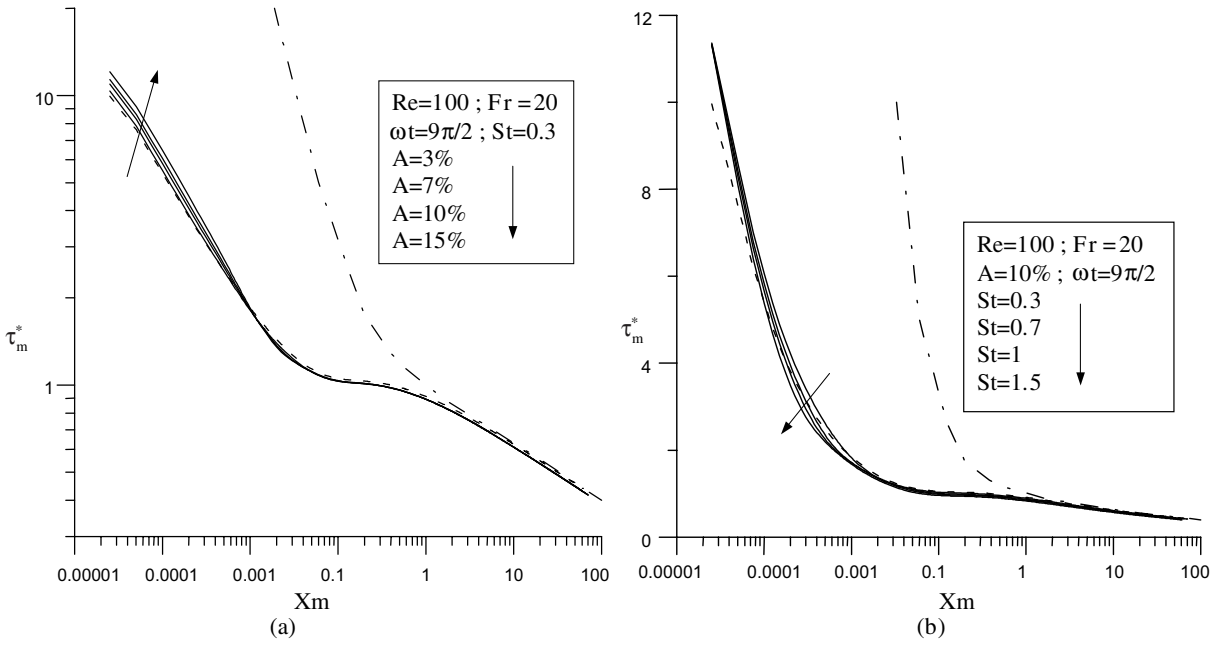

Fig. 12. Longitudinal distribution of the modified shear stress: (a) influence of pulse amplitude, (b) influence of Strouhal number; - - - results of [21], –·–·–·– results of [26].

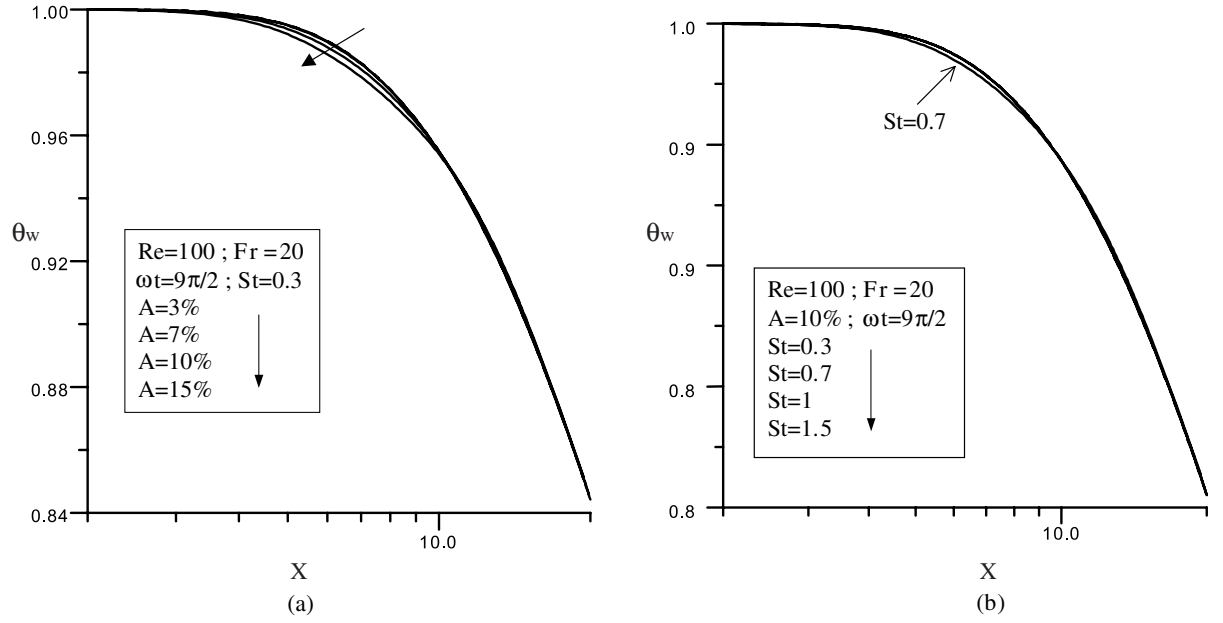

Fig. 13. Longitudinal distribution of the wall temperature: (a) influence of pulse amplitude, (b) influence of Strouhal number; - - - results of [21], –·–·–·– results of [26].

jet and the ambient conditions. On the other hand a variation, of the pulsation frequency acts little on the wall temperature since a light jet cooling is observed only for one Strouhal number equal to 0.7 (Fig. 13(b)). In addition to that and compared with the pulsed free jet case and for the same parameters, it is noticed that the fluctuations of the temperature (Fig. 11) are more important, this makes us to think that the wall tends to

reduce the effect of the ejection velocity oscillations on the flow.

3.2.2. Wall subjected to a constant temperature

We have also studied numerically, the parietal pulsed jet case in a laminar regime, tangentially developing to a wall subjected to a constant temperature which is equal to the one at the exit nozzle jet.

The influence of the parameters related to the pulsation (amplitude of pulsation and a Strouhal number) on the heat transfer between the heated wall and the pulsed plane jet is also analyzed. The physical parameter which characterizes the heat transfer is the dimensionless local Nusselt number defined by

$$Nu = \frac{hx}{\lambda} = -X \left.\frac{\partial \theta}{\partial Y}\right|_{Y=0} \tag{10}$$

We present thus on Fig. 14(a), the longitudinal variation of local Nusselt number for various pulsation amplitudes. The results found for $Re = 100$, $Fr = 20$ and $St = 0.3$ are compared with those established for the permanent jet. It is also noticed that the Nusselt number increases with the pulsation amplitude. The increase in the heat transfer between the wall and the pulsed jet is observed in a region located between the nozzle and $X \approx 7$. Indeed in this zone located in the nozzle vicinity, the increase in the pulsation amplitude produces for $\omega t = 9\pi/2$ more important ejection velocity than that of the permanent jet, this acceleration associated with a higher entrainment of the surrounding air makes an increase on the heat exchange between the wall and the jet. This result was already announced by Farrington and Claunch [13] in a pulsed plane air jet case. From $X \approx 7$ the pulsation does not effect the heat transfer in the wall.

We present on Fig. 14(b), the effect of the Strouhal number on the Nusselt number for $Re = 100$, $Fr = 20$ and $A = 10\%$. The effect of the pulsation on the parietal jet with great Strouhal numbers bring a contribution to the increase in the heat exchange at the wall on a region which extends to $X \approx 1.3$ for $St = 2$ and to $X \approx 2$ for $St = 1$. On the other hand, for the low pulsation frequencies, the heat exchanges are more important than those relative to the permanent jet on a wider zone which reaches $X \approx 7$ for $St = 0.3$. Beyond this distance, the evolutions of the Nusselt number for the pulsed jet are merged with that established for the permanent jet, thus we reach an equivalent exchange regime as the permanent jet for the various Strouhal numbers values.

For better quantifying the influence of the disturbance on thermal exchange with the wall, we have to analyze the effect of the pulsation on the average Nusselt number defined by

$$\overline{Nu} = \frac{1}{L}\int_0^L Nu \cdot \mathrm{d}x = \frac{1}{L}\int_0^L \frac{hx}{\lambda}\,\mathrm{d}x = -\frac{1}{L}\int_0^L \left.\frac{\partial \theta}{\partial Y}\right|_{Y=0} X\,\mathrm{d}X \tag{11}$$

Since Fig. 15 shows us that the thermal exchange with the wall are affected by the pulsation only in one region located between the nozzle and $X \cong 7$, the distance L is fixed at this already mentioned value.

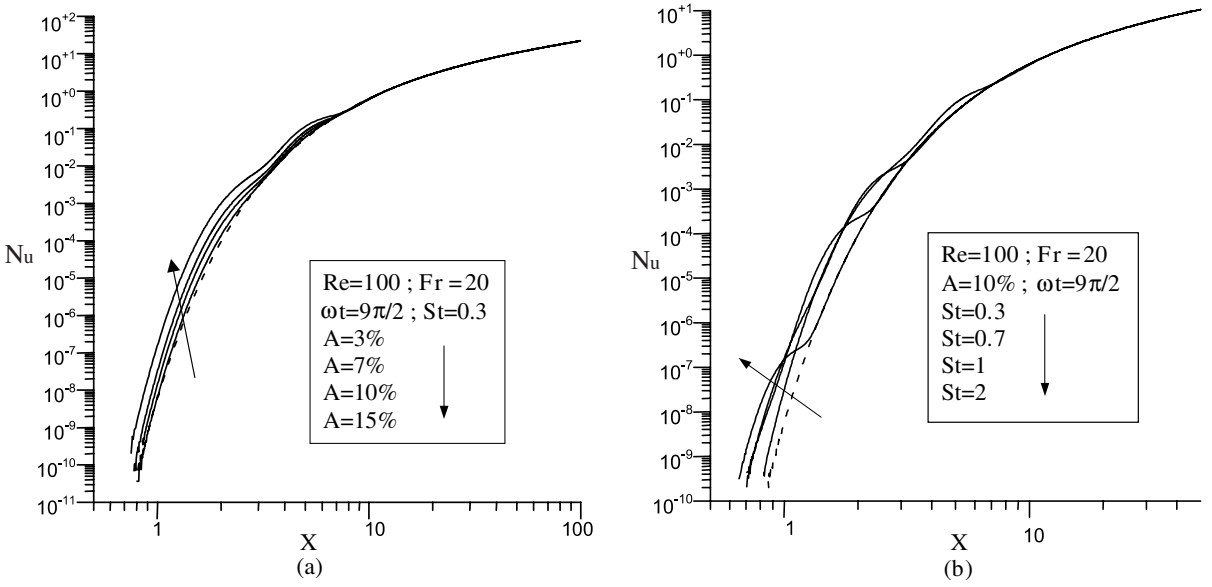

Fig. 14. Longitudinal distribution of the local Nusselt number: (a) influence of pulse amplitude, (b) influence of Strouhal number; - - - steady jet.

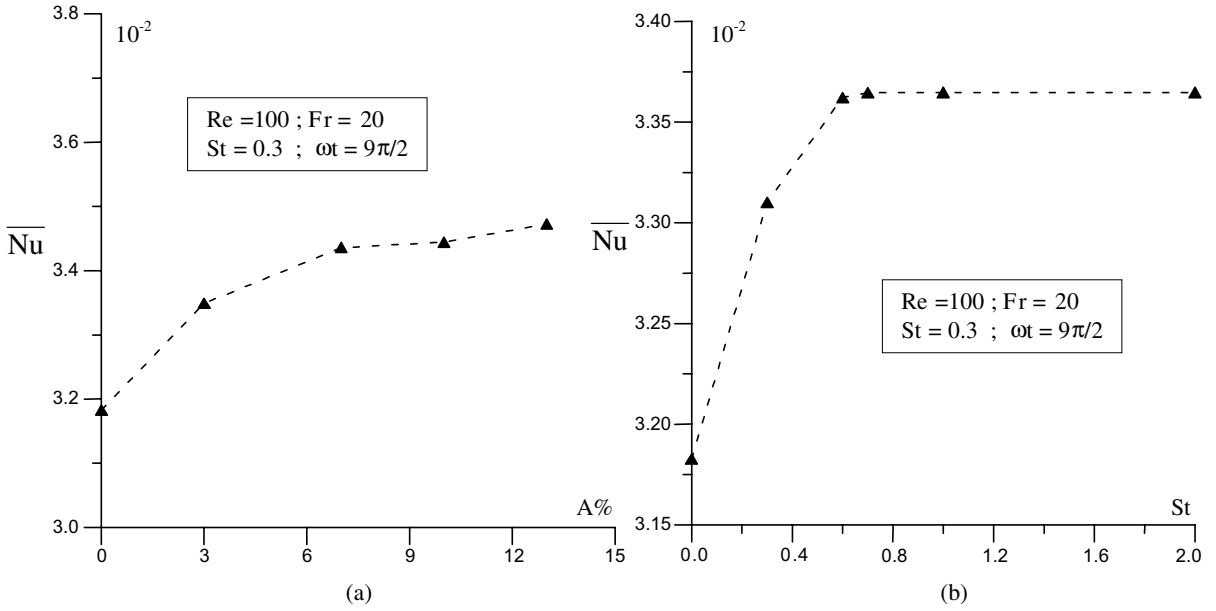

Fig. 15. Average Nusselt number according to the: (a) pulsation amplitude, (b) Strouhal number.

The average Nusselt number is presented according to the pulsation amplitude for a fixed Strouhal number $St = 0.3$ (Fig. 15(a)) and according to Strouhal numbers for a pulsation amplitude of $A = 10\%$ (Fig. 15(b)). Fig. 15(a) enables us to confirm that an increase in the pulsation amplitude involves an increase in the heat exchange at the wall, indeed an amplitude of pulsation of 10% involves an increase in the thermal transfer of 8% compared to the permanent jet. On the other hand, we notice on Fig. 15(b) an abrupt increase in the thermal transfer for $St = 0.3$ and beyond a pulsation frequency corresponding to a Strouhal number of 0.6, the pulsation does not influence any more the thermal exchange at the wall and the increase of the average Nusselt number is about 9% for the all considered Strouhal numbers.

4. Conclusion

In this work, we have studied an unsteady and in a laminar regime the momentum and the heat transfer in a free and parietal vertical plane jet subjected to a sinusoidal disturbance. The numerical resolution of the equations was carried out by a numerical method with the finite differences using a staggered grid.

The carried discussion is essentially about the validity of our calculation code elaborated to describe the dynamic and the thermal quantities of this flow type, and the influence of the parameters which describe the pulsation, in particular the amplitude of pulsation and the Strouhal number, on the characteristics of the pulsed jet.

The temporal evolution of the principal flow parameters for various pulsation amplitudes enabled us to notice that there is a non-periodic part (flat) which depends on the distance to the nozzle, and a periodic part which attenuated according to time and space. For the low Strouhal numbers, the centerlines velocity and the temperature keep a sinusoidal profile on very high distances to the nozzle. On the other hand, for the high pulsation frequencies the sinusoidal structure of the flow is of low amplitude and quickly loses its identity under the effect of the molecular viscosity.

The spatial evolution of the characteristic quantities of the flow at a fixed instant enables us to notice the rapidity with which the pulsation develops the jet in the region close to the nozzle. On the other hand, the variation of the amplitude or the frequency of the pulsation does not affect in any case the characteristics of the flow in the plume region. This phenomenon was observed already by Acton [27] and Chan [28] in the case of a disturbed axisymmetric jet.

The development of the pulsed jet thus depends at the same time on both the pulsation amplitude and on the Strouhal number and it is difficult to separate their respective influences, but in all cases, the pulsed jet reaches the same equilibrium regime as the permanent jet in the plume region. In this latter our results agree very well with the results established by Mhiri et al. [21] and Yu et al. [26].

For a parietal pulsed jet, two thermal conditions at the wall are considered: first adiabatic wall, second the wall subjected to a constant temperature. We have noticed a good agreement between our results and those

obtained by Yu et al. [26] and Mhiri et al. [21] in the plume region (far from the nozzle), the effect of the pulsation being observed only on the jet and intermediary regions.

The increase in the average Nusselt number was estimated at 8% for a pulsation amplitude of 10% and for Strouhal number equal to 0.3. In addition, for all the high pulsation frequencies ($\geqslant 6\%$) the increase in the thermal transfer is estimated at 9%.

To close this work it is important to say that the pulsation does not modify the flow parameters in the region of the established regime (plume region), but it does accelerate the initial development of the jet and improve the diffusion and the entrainment in the first diameters.

References

[1] Phénomènes thermiques et hydrauliques non stationnaires, Conférences C.E.A., E.D.F., Jouy en Josas, Proc. Eyrolles Editeur, 1976.

[2] M. Favre-Marinet, G. Binder, Structure des jets pulsants, J. Mech. 18 (1978) 355–394.

[3] A.K.M.F. Hussain, A. Rayclark, Upstream influence on the near field of plane turbulent jet, Phys. Fluid 20 (9) (1977) 1416–1426.

[4] A.K.M.F. Hussain, C.A. Thompson, Controlled symmetric perturbation of the plane jet an experimental study in initial region, J. Fluid Mech. 100 (2) (1980) 397–431.

[5] W.G. Hill, P.R. Greene, Increased turbulent jet mixing rates obtained by self excited acoustic oscillations, J. Fluids Eng. 99 (3) (1977) 520–525.

[6] R.M. Curtet, J.P. Girard, Visualization of a pulsating jet, in: Proceedings of the Symposium on Fluid Mechanics of Mixing, ASME, New York, 1973.

[7] S.C. Crow, F.H. Champagne, Orderly structure in jet turbulence, J. Fluid Mech. 48 (1971) 547–591.

[8] D. Bechert, E. Pfizenmaier, On wavelike perturbations in a free jet travelling faster than the mean flow in the jet, J. Fluid Mech. 72 (1975) 341–352.

[9] E.C. Mladin, D.A. Zumbrunnen, Local convective heat transfer to submerged pulsating jets, Int J. Heat Mass Transfer 40 (14) (1997) 3305–3321.

[10] K.B.M.Q. Zaman, A.K.M.F. Hussain, Vortex pairing in a circular jet under controlled excitation, part 1. General jet response, J. Fluid Mech. 101 (3) (1980) 449–491.

[11] A.K.M.F. Hussain, K.B.M.Q. Zaman, Vortex pairing in a circular jet under controlled excitation, part 2. Coherent structure dynamics, J. Fluid Mech. 101 (3) (1980) 493–544.

[12] F.B. Hsiao, J.M. Huang, On the dynamics of flow structure development in an excited plane jet, Trans. ASME 116 (1994) 714–720.

[13] R.B. Farrington, S.D. Claunch, Infrared imaging of large-amplitude, low-frequency disturbances on a planar jet, AIAA J. 32 (1994) 317–323.

[14] C.O. Popiel, O. Trass, Visualization of a free and impinging round jet, Exp. Thermal Fluid Sci. 4 (1991) 253–264.

[15] R.G. Nevins, H.D. Ball, Heat transfer between a flat plate and a pulsating impinging jet, in: Proceedings of the National Heat Transfer Conference, Boulder, CO, vol. 60, ASME, New York, 1961, pp. 510–516.

[16] D.A. Zumbrunnen, M. Aziz, Convective heat transfer enhancement due to the intermittency in an impinging jet, J. Heat Transfer 115 (1993) 91–98.

[17] H.S. Sheriff, D.A. Zumbrunnen, Effect of flow pulsations on the cooling effectiveness of an impinging planar water jet, J. Heat Transfer 116 (1994) 886–895.

[18] L.F.A. Azevedo, B.W. Webb, M. Queiroz, Pulsed air jet impingement heat transfer, Exp. Thermal Fluid Sci. 8 (1994) 206–213.

[19] M.D. Zhou, C. Heine, I. Wygnanski, The effects of excitation on the coherent and random motion in a plane wall jet, J. Fluid Mech. 310 (1996) 1–37.

[20] V.S. Patankar, Numerical heat transfer and fluid flow, Hemisphere publishing corporation, New York, 1980, pp. 106.

[21] H. Mhiri, S. El Golli, G. Le Palec, P. Bournot, Influence des conditions d'émission sur un écoulement de type jet plan laminaire isotherme ou chauffé, Rev. Générale Thermiques, Ed. Elsevier 37 (1998) 898–910.

[22] H. Mhiri, S. Habli, S. El Golli, G. Le Palec, P. Bournot, Etude numérique des conditions d'émission sur un écoulement de type jet plan turbulent isotherme ou chauffé, Int. J. Thermal Sci. 38 (1999) 904–915.

[23] A.M. Dalbert, F. Penot, J.L. Peube, Convection naturelle laminaire dans un canal vertical chauffé à flux constant, Int. J. Heat Mass Transfer 24 (1981) 1453–1473.

[24] R. Siegel, M. Perlmutter, Heat transfer for pulsating laminar duct flow, Trans. ASME J. Heat Transfer 84 (2) (1962) 111–123.

[25] R. Siegel, Influence of oscillation-induced diffusion on heat transfer in a uniformly heated channel, Trans. ASME J. Heat Transfer 109 (1987) 244–247.

[26] W.S. Yu, H.T. Lin, H.C. Shih, Rigorous numerical solutions and correlation for two dimensional laminar buoyant jets, Int. J. Heat Mass Transfer 35 (5) (1992) 1131–1141.

[27] E. Acton, A modelling of large eddies in axisymmetric jet, J. Fluid Mech. 98 (1) (1980) 1–31.

[28] Y.Y. Chan, Spatial waves in turbulent jets, Phys. Fluids 17 (1974) 46–53.